# Interior Magnetic Fields in Magnetars

*3D GRMHD Simulations of Rotating Neutron Stars*

Raj Kishor Joshi[1] ,William Cook[2], Brynmor Haskell[3] , Sebastiano Bernuzzi[2]

1-CAMK, Warsaw, Poland
2-FSU Jena
3- Università degli Studi di Milano

MERLIN project
The Magnetic Field Dynamics in Neutron Stars

# Talk Outline

**01** **Motivation & Open Questions**

*Why internal B-field topology matters*

**02** **Numerical Setup**

*AthenaK GRMHD, initial conditions, diagnostics*

**03** **Two Evolutionary Regimes**

*The Lehnert number criterion Le = P/τ_A*

**04** **Physical Mechanisms**

*Differential rotation, Ω-dynamo, helicity, turbulence*

**05** **Pulsar Population**

*P-Ṗ diagram & observational implications*

**06** **Gravitational Waves**

*Mode excitation, nonlinear coupling, GW signatures*

**07** **Summary**

*Key results & future directions*

MOTIVATION

# Neutron Star Magnetic Fields: A Central Open Question

## What we know

- B up to $10^{15}$ G in magnetars
- Magnetic deformation
- Pulsar timing → large-scale dipole near light cylinder
- NICER reveals rich multipolar structure near surface

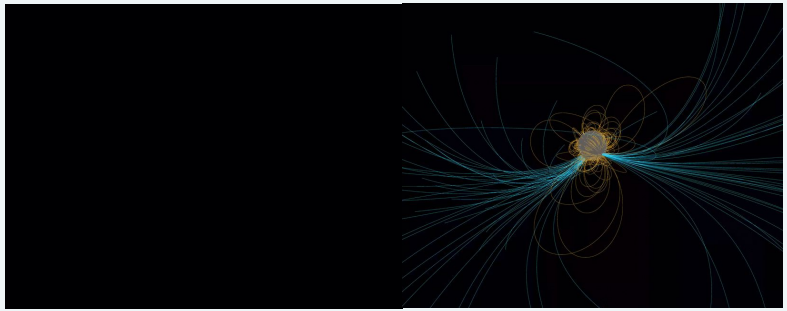

NICER observations from July 2017 to December 2018, for J0030

## What we don't know

- Internal field topology — poloidal? toroidal? mixed?
- Relative strength of toroidal vs poloidal components
- Role of rotation in setting field geometry
- Long-term stability and secular evolution

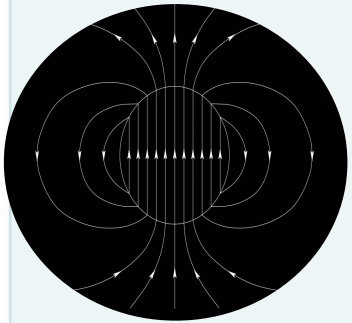

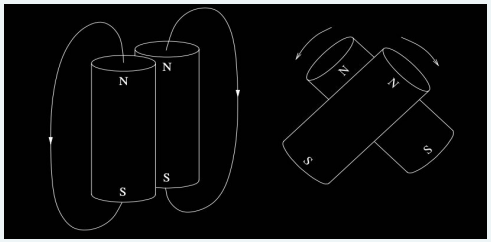


**Key gap: how does rotation compete with magnetic stresses to set the internal field structure?**

# Previous Simulations & The Missing Ingredient

- Braithwaite & Spruit (2004), Sur et al. (2020, 2021), Cook et al. (2025): purely poloidal/toroidal fields are unstable on the Alfvén timescale.
- Kink instability of the poloidal field (Markey & Tayler 1973) and Tayler instability of toroidal field drive system toward mixed poloidal–toroidal configurations
- Turbulence plays a key role in helicity transfer and large-scale field organisation.
- Twisted-torus configurations have been proposed as the stable geometry — but conditions for their realisation are debated.

Missing ingredient: rotation. Only a handful of studies have explored field evolution in rotating systems — none in the **low Lehnert number** regime directly relevant to most pulsars.

NUMERICAL SETUP

# Role of timescales & Lehnert Number

### The Lehnert Number

$$\mathrm{Le} \equiv P / \tau_A \quad \text{where} \quad \tau_A = 2R\sqrt{\langle\rho\rangle} / \langle B\rangle$$

*Le < 1 → rotationally dominated | Le > 1 → magnetically dominated*

### Rotation-modified instability timescale (Pitts & Tayler 1985)

$$\tau_{\mathrm{rot}} = \tau_A^{\,2} / P = \tau_A / \mathrm{Le}$$

For Le < 1: Coriolis force stretches the instability timescale by 1/Le → rotation suppresses kink instability

| $P$ (ms) | $B_1 \times 10^{15}$G | $B_2 \times 10^{15}$G | Le | |
|---|---|---|---|---|
| | | | $B_1$ | $B_2$ |
| 1.63 | 8.15 | 40.77 | 0.12 | 0.64 |
| 2.39 | 11.09 | 44.39 | 0.23 | 0.91 |
| 10.84 | 12.94 | 2.58 | 0.88 | 0.20 |
| 20.52 | 13.00 | 2.60 | 2.08 | 0.41 |
| 50.00 | 13.02 | 1.30 | 5.22 | 0.52 |

NUMERICAL SETUP

# AthenaK GRMHD: Code & Initial Conditions

## Code: AthenaK

- 3D ideal GRMHD in dynamical spacetime
- Z4c formulation of Einstein equations
- PPMX reconstruction + HLLE Riemann solver
- 3rd-order SSP Runge–Kutta time evolution
- Upwind constrained transport for $\nabla \cdot B = 0$
- Block-structured statically refined grid, ±480 km domain
- Resolutions: 450m, **230m**, 110m (HR)

## Initial Conditions

- Polytropic EOS: N=1, K=100
- AU sequence (Dimmelmeier+ 2006): $AU_1$–$AU_5$ fast rotators (T = 1.63–2.39 ms)
- $S_1$–$S_3$ slow rotators (T = 50 ms-10.84ms)
- Fixed rest mass $M_0 = 1.506\ M_\odot$
- Purely poloidal initial field
- $B_1$ series: fixed B field
- $B_2$ series: scaled field to straddle Le = 1 boundary

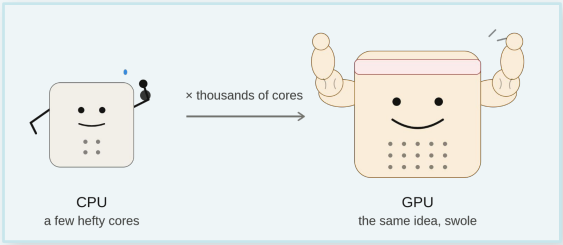


Publically available at:
https://github.com/IAS-Astrophysics/athenak

Longest (1.2s) & Highest resolution (29m) to date W. Cook et al. 2026 MNRAS 547, 1–11

## RESULTS: FIELD STRUCTURE

**P=2.39ms**

Time=24.625 ms

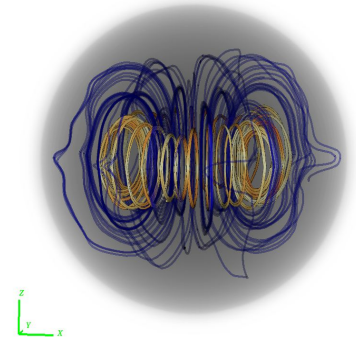

Time=35.46 ms

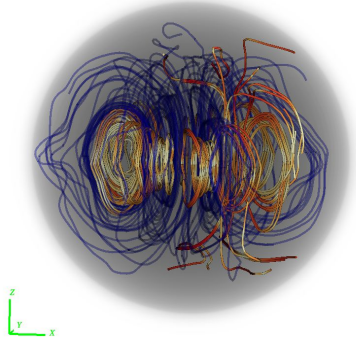

Time=53.19 ms

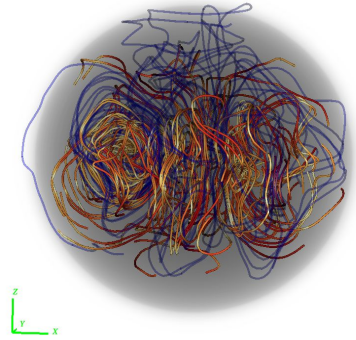

Time=100.962 ms

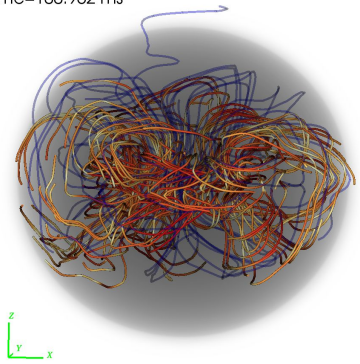

Time=24.1325 ms

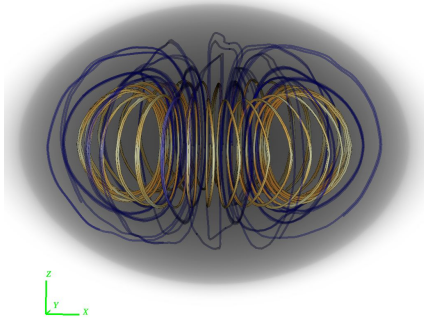

Time=35.46 ms

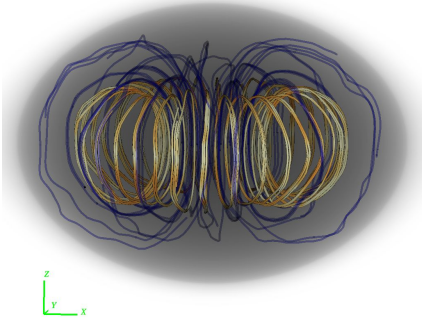

Time=59.1 ms

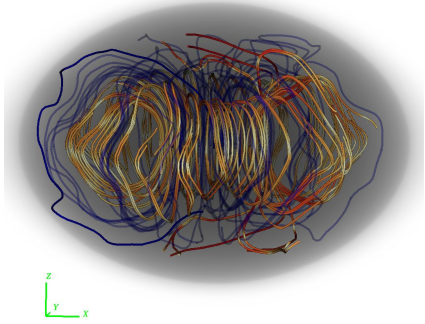

Time=103.425 ms

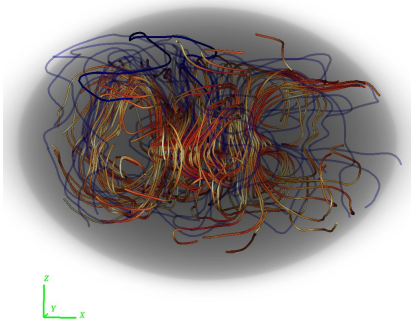

**P=1.**

# Two Evolutionary Regimes: Magnetic Energy Evolution

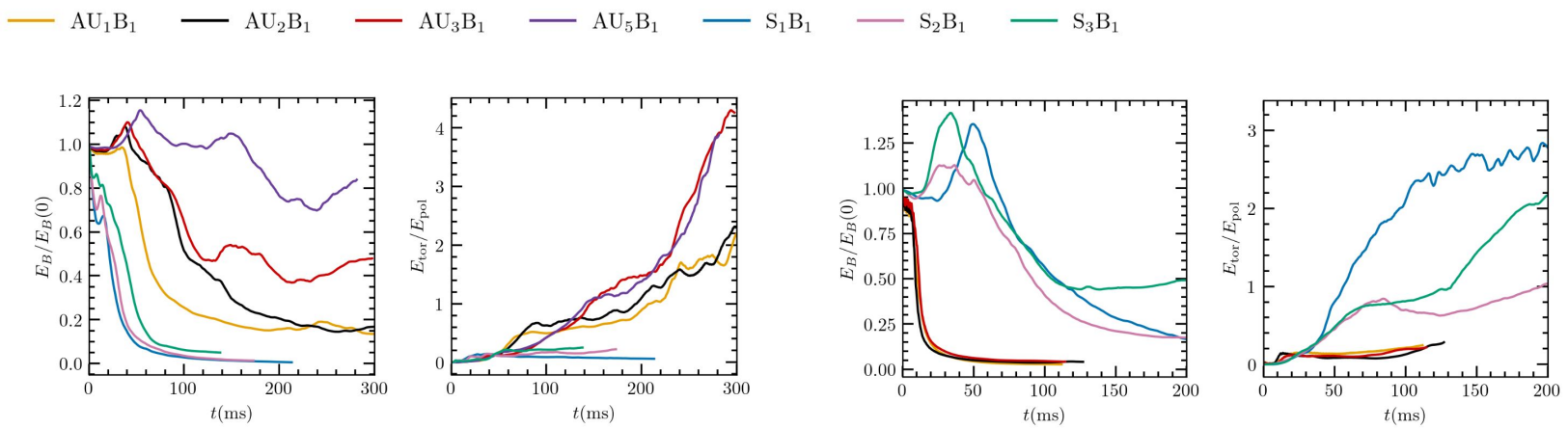


Le < 1 (rotation dominated): field retained, E_tor ≥ E_pol, stable over 10–15 T_A

Le > 1 (magnetically dominated): >90% field lost within 100 ms, E_tor ~ 6–25% only

# Two Distinct End States: 3D Field Line Structure

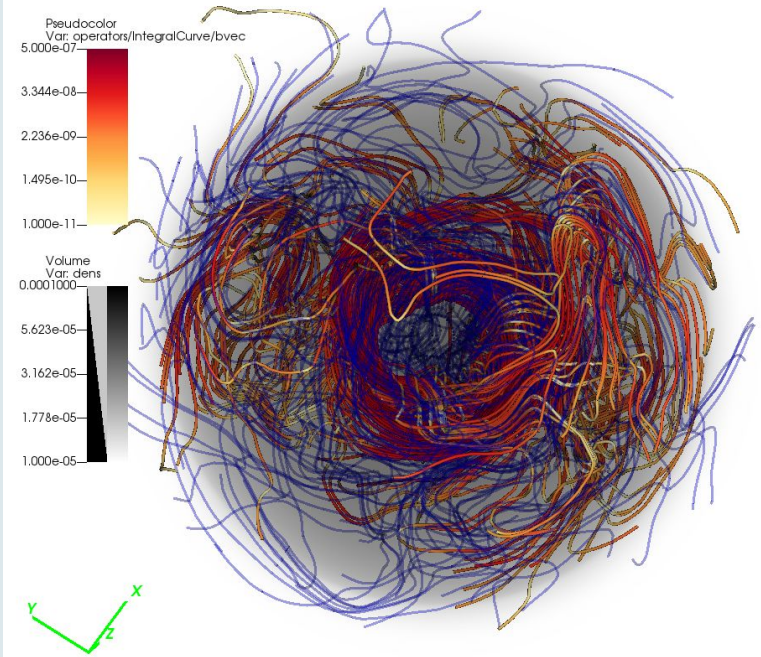


**Le < 1 → Coherent twisted-torus, strong toroidal winding**

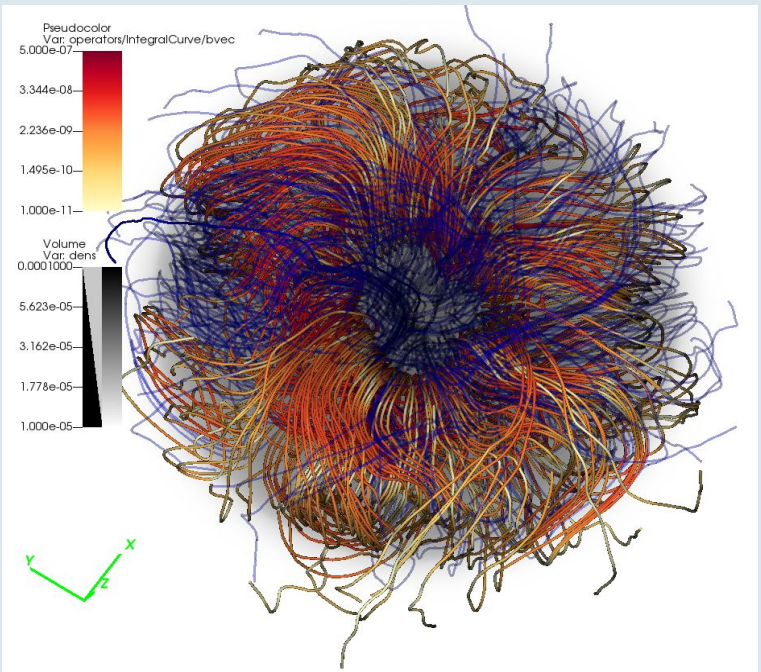


**Le > 1 → Weak toroidal, dominant poloidal**

*Field lines seeded at r = 4.5 km, colour-coded by $B_{\varphi}^2$. Blue lines (poloidal) seeded near stellar core. Snapshot at $T_A \sim 15$.*

# Physical Mechanism: The Ω-Dynamo and Differential Rotation

**Ω-dynamo equation:**

$$dB_\varphi/dt = q\,\Omega\,B_p - B_\varphi / \tau_{rot}$$

*where* $\tau_{rot} = \tau_A^2 / P = \tau_A / Le$

**Forcing term: qΩBp**

Differential rotation winds poloidal B into toroidal.

**Damping term: $B_\varphi/\tau\_rot$**

Le < 1 → $\tau_{rot} = \tau_A/Le \gg \tau_A$ → damping is slow → toroidal field grows. Le > 1 → $\tau_{rot} \sim \tau_A$ → damping fast → instability wins.

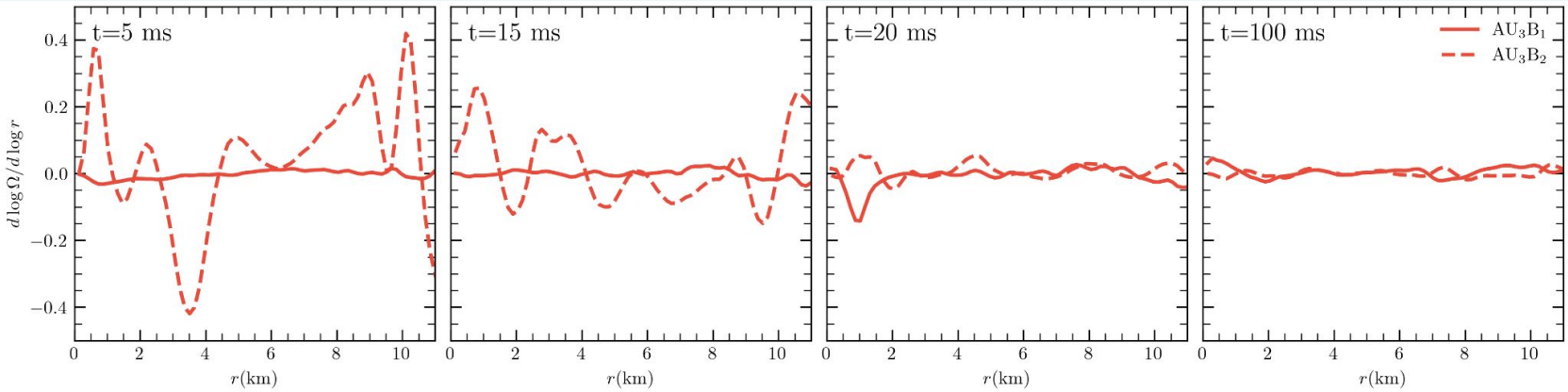

# Physical Mechanism: The Ω-Dynamo and Differential Rotation

**Ω-dynamo equation:**

$$dB_\varphi/dt = q\,\Omega\,B_p - B_\varphi / \tau_{rot}$$

*where* $\tau_{rot} = \tau_A^2 / P = \tau_A / Le$

**Forcing term: qΩBp**

Differential rotation winds poloidal B into toroidal.

**Damping term: B_φ/τ_rot**

Le < 1 ⟶ τ_rot = τ_A/Le ≫ τ_A ⟶ damping is slow ⟶ toroidal field grows. Le > 1 ⟶ τ_rot ~ τ_A ⟶ damping fast ⟶ instability wins.

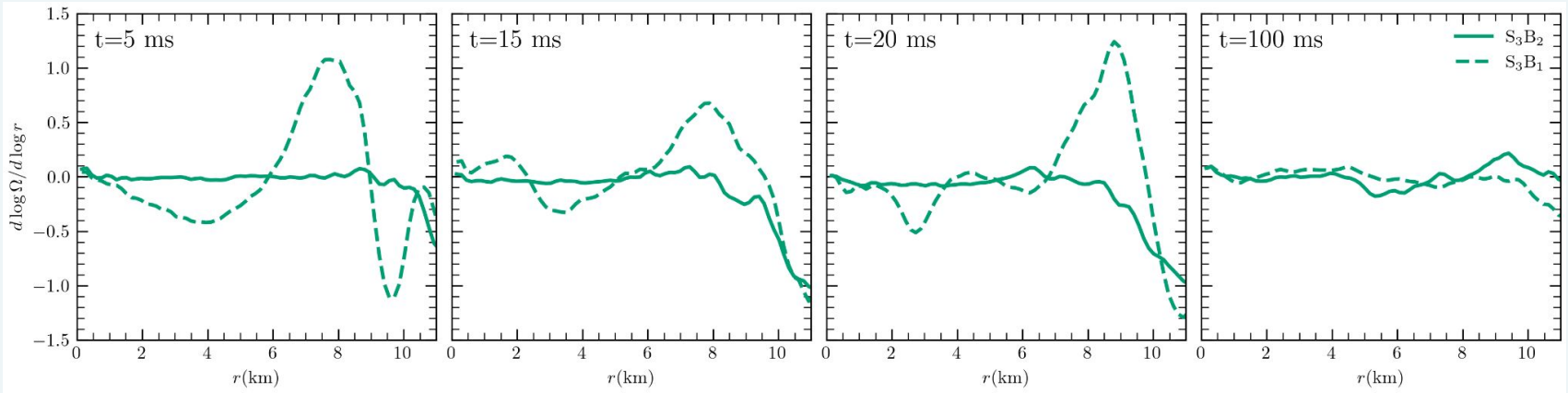

# Physical Mechanism: The Ω-Dynamo and Differential Rotation

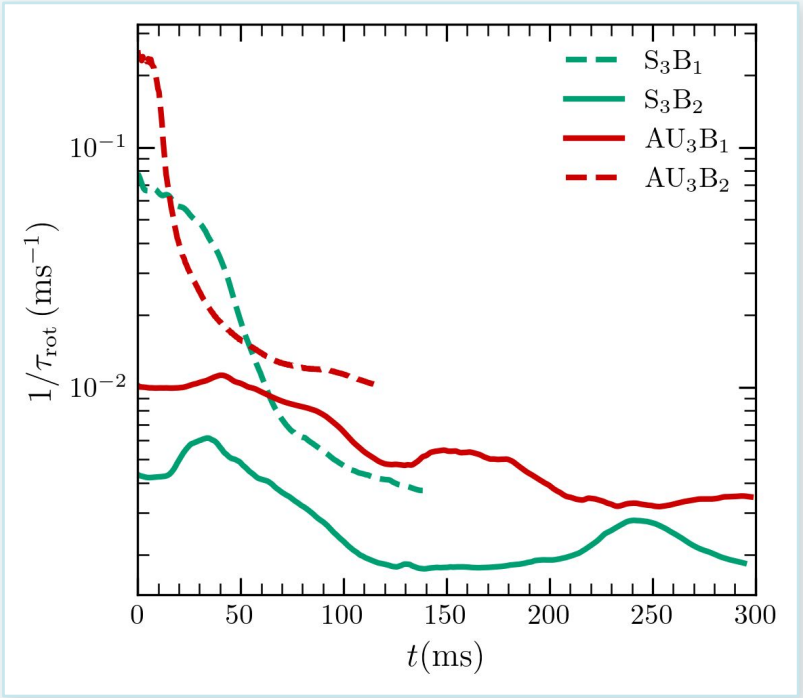


**Forcing term: qΩBp**

Differential rotation winds poloidal B into toroidal.

**Damping term: B_φ/τ_rot**

Le < 1 → τ_rot = τ_A/Le ≫ τ_A → damping is slow → toroidal field grows. Le > 1 → τ_rot ~ τ_A → damping fast → instability wins.

**Topological protection**

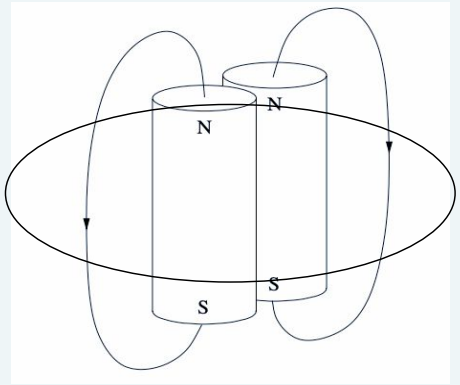

# Magnetic Helicity: Building Topological Protection

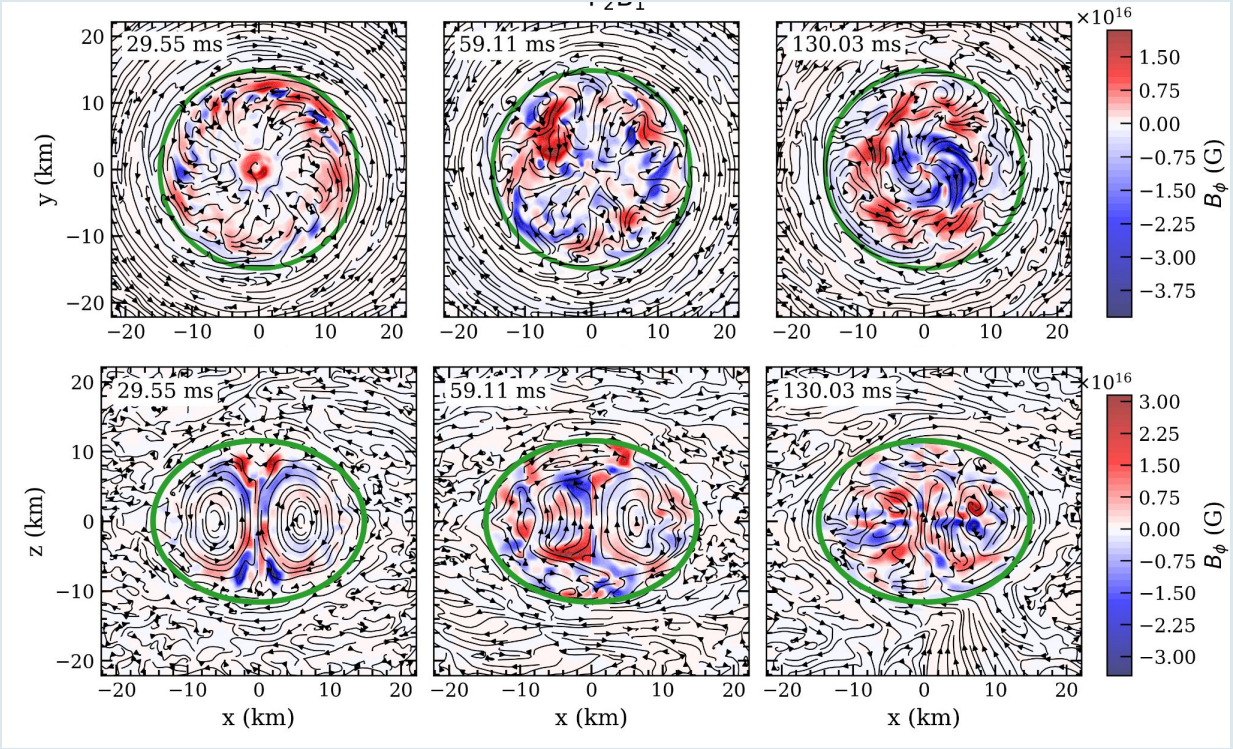


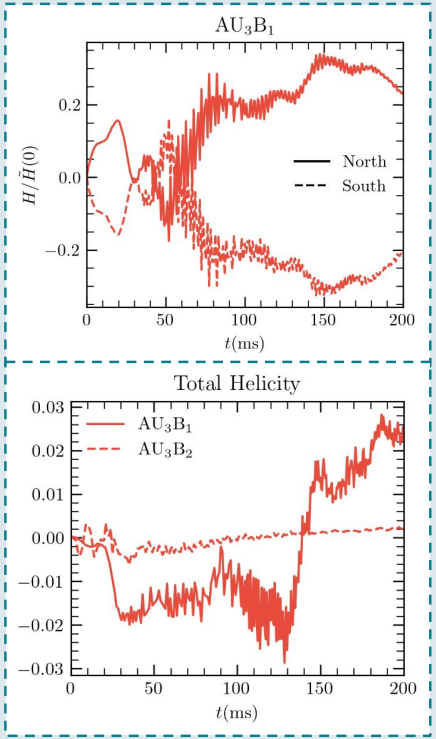

RESULTS: HELICITY

# Magnetic Helicity: Building Topological Protection

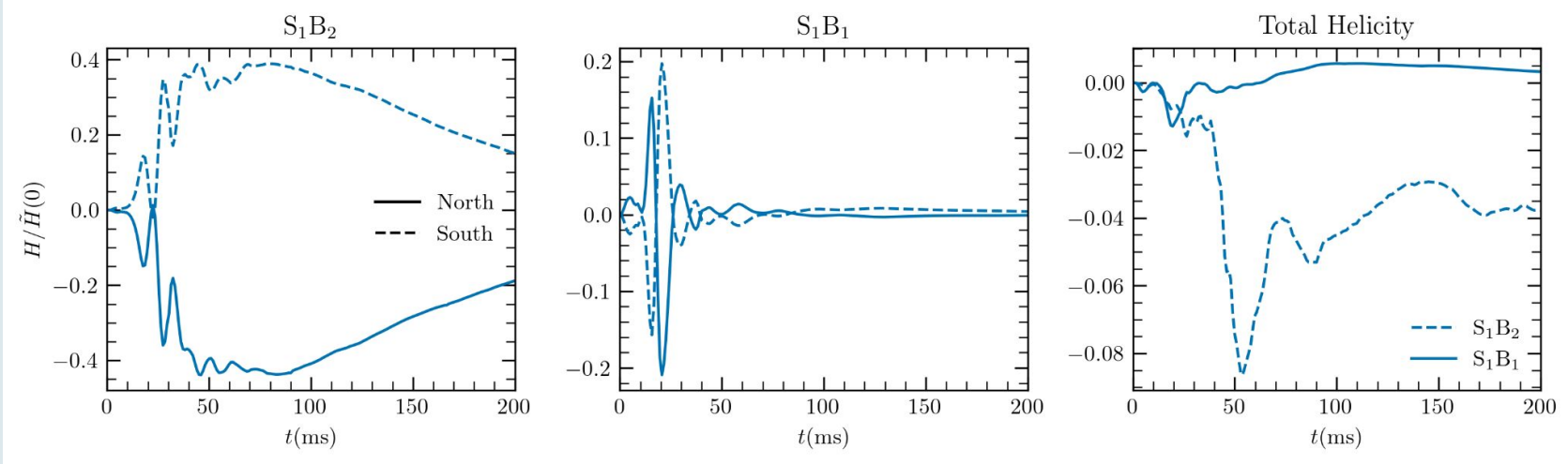


Le < 1: Differential winding builds hemispheric antisymmetry → kink instability → net helicity with preferred handedness → sustained oscillations. Topological protection halts further decay.

Le > 1: Only transient helicity signal — poloidal field decays rapidly into weak toroidal component. No sustained winding → helicity damps → no topological protection.

RESULTS: TURBULENCE

# Magnetic Power Spectra

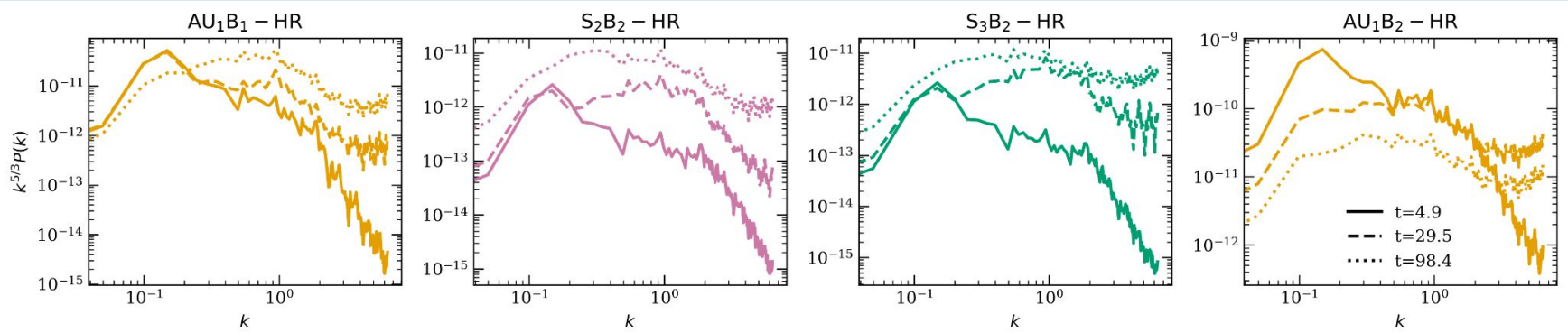


**flat compensated Kolmogorov-like turbulence. Need more resolution for capture it Cook et. al. 2026 See William Cook's talk**

### $AU_1B_1$ (fast, Le<1)

Low-k power decreases (Tayler disrupts large-scale field) while high-k power grows (differential winding redistributes energy). Flat compensated spectrum at intermediate k.

### $S_2B_2$, $S_3B_2$ (slow, Le<1)

Power grows across all scales including low-k — corresponds directly to transient energy growth seen in energetics.

### $AU_1B_2$ (Le>1)

Monotonic power decrease across ALL scales by ~2 orders of magnitude. No flat inertial range — no turbulent cascade. Pure decay driven by Tayler instability.

PULSAR POPULATION

# Mapping Le = 1 onto the P–Ṗ Diagram

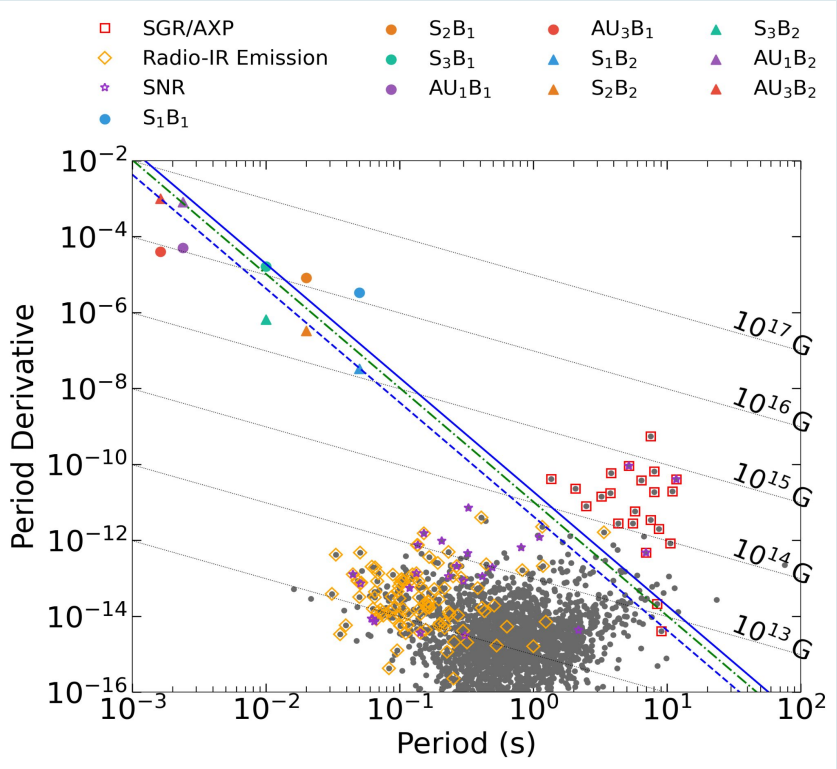


## The criterion

$$\tau_A = P \rightarrow \alpha/B = P$$

*α = 1.03 × 10¹⁴ (from simulations)*

$$B \approx 3.2 \times 10^{19} \sqrt{P\dot{P}}\,\mathrm{G}$$

- Above boundary (Le>1): Magnetically dominated → mostly magnetars → quasi-poloidal fields
- Below boundary (Le<1): Rotationally dominated → majority of radio pulsars → strong toroidal interior
- Low-field magnetars (SGR J1822, SGR 0418) near boundary.

PULSAR POPULATION

# Mapping Le = 1 onto the P–Ṗ Diagram

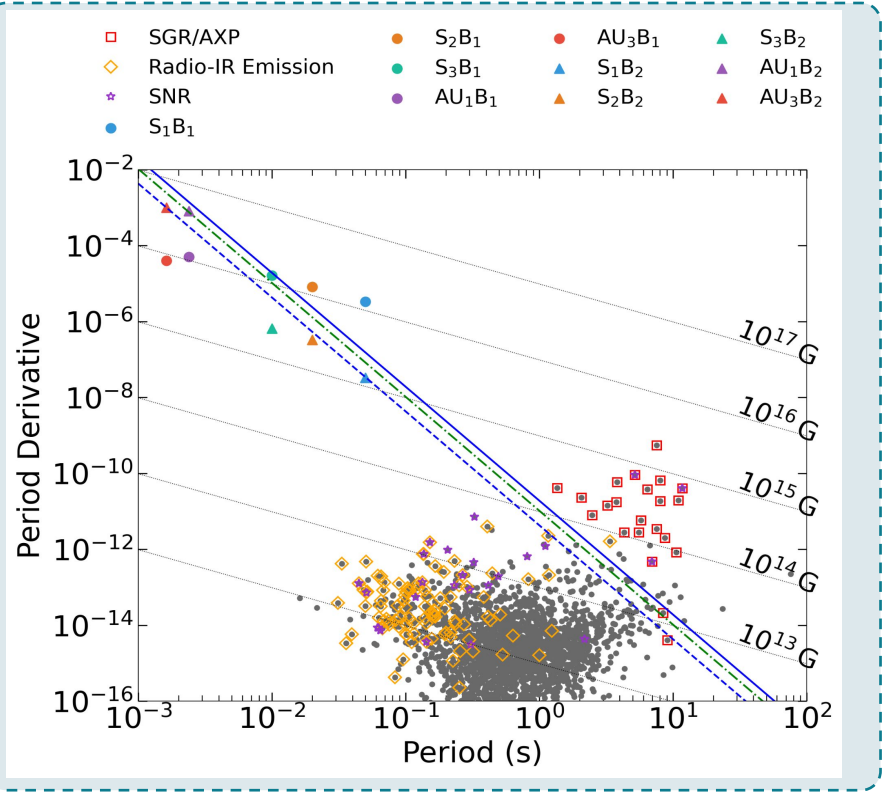


## Magnetars (Le > 1)

- Predominantly poloidal internal field
- Active Tayler instability → continuous field decay → SGR/AXP bursting activity
- Low-field magnetars: born as Le<1, wound up strong toroidal, differential rotation decayed → became magnetically dominated → bursting
- Differences between magnetars may reflect progenitor differential rotation (SN explosion vs BNS merger)

## Radio Pulsars (Le < 1)

- Strong internal toroidal field — possibly up to 10× the exterior dipole inferred from spin-down
- A mixed poloidal–toroidal configuration

GRAVITATIONAL WAVES

# Mode Excitation: PSD of Central Density

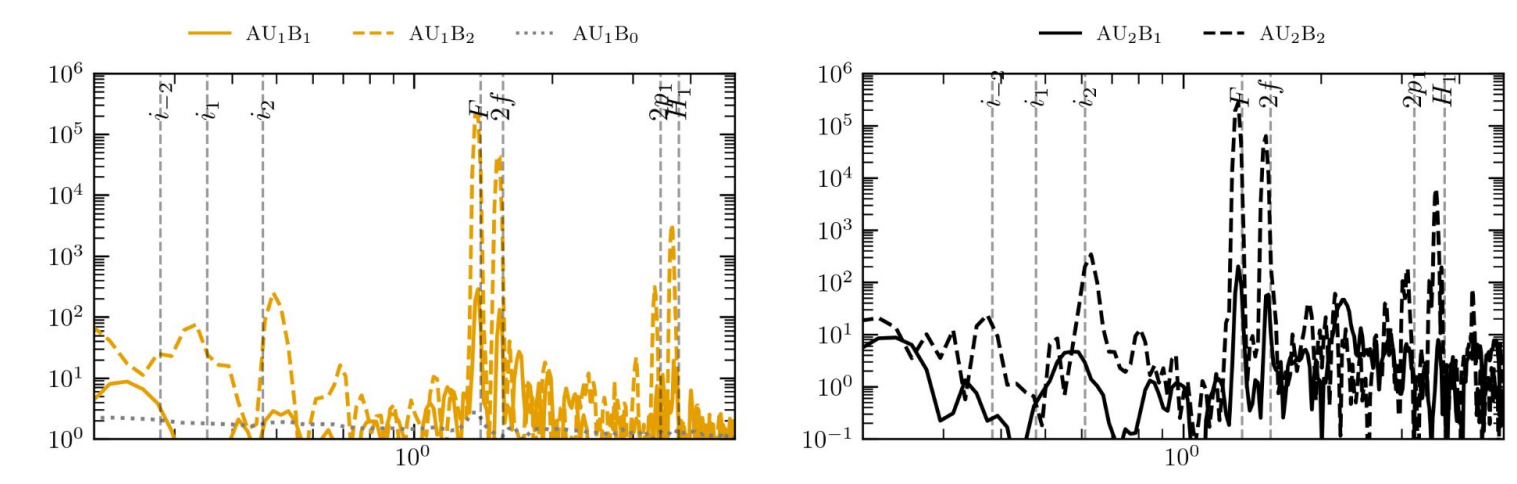


**Magnetically dominated**

Strong broadband excitation. Prominent peaks at F, $^2$f, $2p_1$, $H_1$. Inertial modes ($i_{-2}$, $i_1$, $i_2$) strongly excited by non-axisymmetric Tayler forcing + stronger differential rotation.

**Rotation dominated**

Weak mode excitation — Tayler instability suppressed → weak fluid perturbations

**Hydro baseline (B=0)**

Featureless flat spectrum. Confirms all features in magnetic runs are instability-driven, not numerical artifacts.

GRAVITATIONAL WAVES

# Gravitational Wave Emission

### $|\tilde{\Psi}_4^{2,0}|^2$: Axisymmetric quadrupolar GW

Sharp peaks at F, $^2f$, $2p_1$, $H_1$ growing with time and field strength. F peak dominant at early times → $^2f$ dominant at late times (stronger intrinsic quadrupole moment). Hydro baseline flat — confirms magnetic origin.

### $|\tilde{\Psi}_4^{2,2}|^2$: Non-axisymmetric GW — new features

Broadband emission from earliest time → non-axisymmetric Tayler kink modes. Low-f peaks at Ω, 2Ω → magnetic deformation rotating with star (continuous GW!). Novel peak at 1.883 kHz = $^2p_1 - {}^2f$: nonlinear 3-wave combination frequency.

### $^2p_1 - {}^2f$ = 1.883 kHz: Nonlinear wave coupling

- Proves system is in nonlinear oscillation regime
- Absent in hydro and rotation-dominated cases — unique to magnetically dominated regime

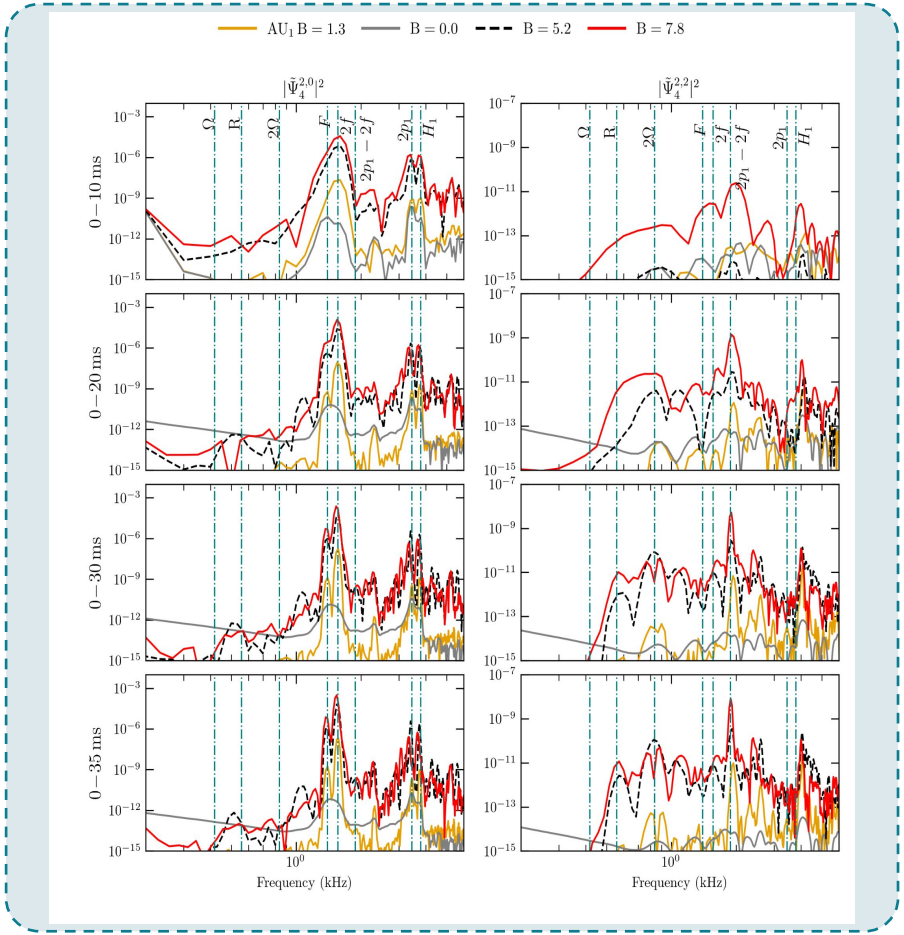

# Gravitational Wave Observational Prospects

## Continuous GWs from magnetic deformation?

Strong hidden toroidal fields in rotation-dominated pulsars → magnetic deformation → continuous quasi-monochromatic GW. Interior B up to 10× exterior dipole → significant signal boost for young pulsars.

## Transient GWs from newly born magnetars

Magnetically dominated regime excites F, $^2f$, $2p_1$, $H_1$ modes. Time-frequency evolution (F multiplet → broadband) is a characteristic signature. Detectable by ET/CE for galactic events. Combination frequency $^2p_1 - {}^2f$ provides EOS constraint.

## Low-field magnetar transitions

Systems transitioning from Le<1 to Le>1 as differential rotation decays (e.g. SGR J1822, SGR 0418). Interesting targets for space-based detectors (DECIGO, BBO) in the sub-20 Hz band (Pagliaro+ 2025).

Next-generation detectors (Einstein Telescope, Cosmic Explorer, DECIGO, BBO) will be able to test these predictions and use the Le=1 criterion as a guide for target selection.

# Summary

*Interior Magnetic Fields in Rotating Neutron Stars*

## 1 Two regimes separated by Le = $P/\tau_A$

Le < 1 ⟶ stable, strong toroidal field via differential winding & helicity protection. Le > 1 ⟶ rapid field decay, weak toroidal component driven by Tayler kink instability.

## 2 Pulsar population prediction

Le=1 boundary on P–$\dot{P}$ diagram: magnetars are magnetically dominated (quasi-poloidal); most radio pulsars are rotation-dominated (strong hidden toroidal B, up to 10× exterior dipole).

## 3 GW signatures

Magnetically dominated stars: rich mode spectrum (F, $^2$f, $H_1$, inertial modes) + novel combination frequency $^2p_1-{}^2$f.

## 4 Turbulence

Rotation-dominated regime hints towards development of Kolmogorov-like turbulence.

# Future Directions & Open Questions

## Physics extensions

- Include exterior fields.
- Differentially rotating initial conditions + magnetic braking — use late-time field config as IC

## Numerical extensions

- Longer duration runs.
- Higher resolution to better resolve MRI and turbulent cascade
- EOS dependence of Le=1 criterion

## Observational connections

- Compute actual GW strain amplitudes for ET/CE target lists
- Use P–$\dot{P}$ boundary to predict internal B for individual sources

## Theoretical work

- Analytic model for toroidal amplification saturation level
- Helicity injection rate as function of Le
- Nonlinear mode coupling rates for $^{2}p_{1}-^{2}f$ combination

**Thank you — Questions welcome**

# Thank You

RESULTS: INSTABILITY DYNAMICS

# Azimuthal Mode Decomposition of the Toroidal Field

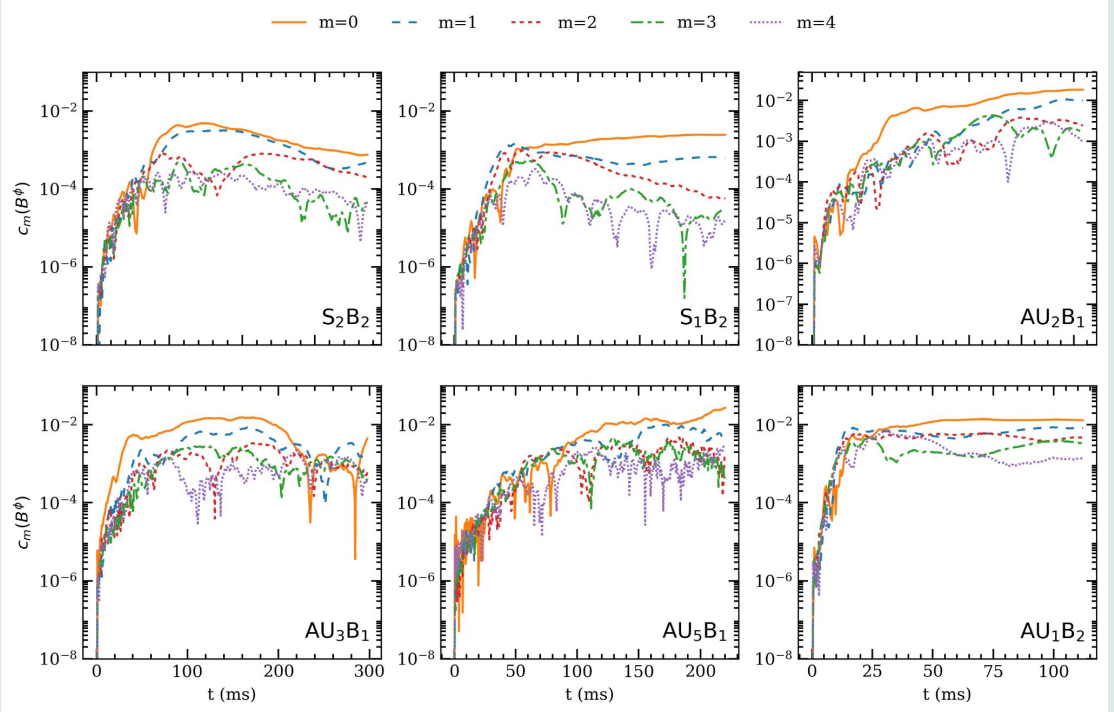


**Slow rotators (Le<1)**

m=0 dominates throughout → coherent axisymmetric winding. Non-axisymmetric modes subdominant.

**Fast rotators (Le<1)**

All modes grow to comparable amplitude — near equipartition. Vigorous non-axisymmetric MHD turbulence driven by rapid winding.

**Magnetically dominated (Le>1)**

m=1 briefly exceeds m=0 at early times → direct signature of Tayler kink instability. All modes then decay together.

# Cowling Approximation vs Full GR: Energy Budget

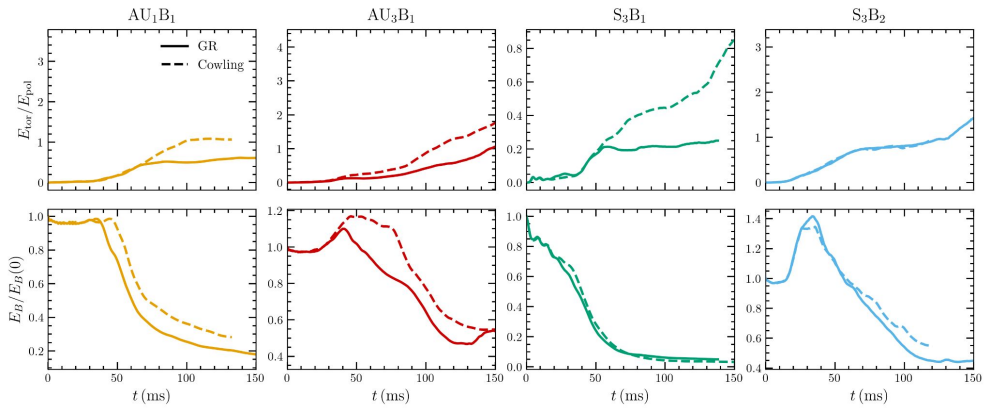


## Key differences

- Cowling overestimates E_tor/E_pol by up to 2×
- Cowling retains more total magnetic energy
- Qualitative regime identification preserved in both
- GR loses extra energy to GW emission — absent in Cowling
- In Cowling: GW energy redirected to differential winding ⟶ stronger toroidal B

Energy budget: ΔE_B ≈ E_KE (Cowling) vs ΔE_B ≈ E_GW + E_KE (GR). GW emission acts as a brake on toroidal field amplification — Cowling systematically overestimates the toroidal component.

# Resolution Convergence Study

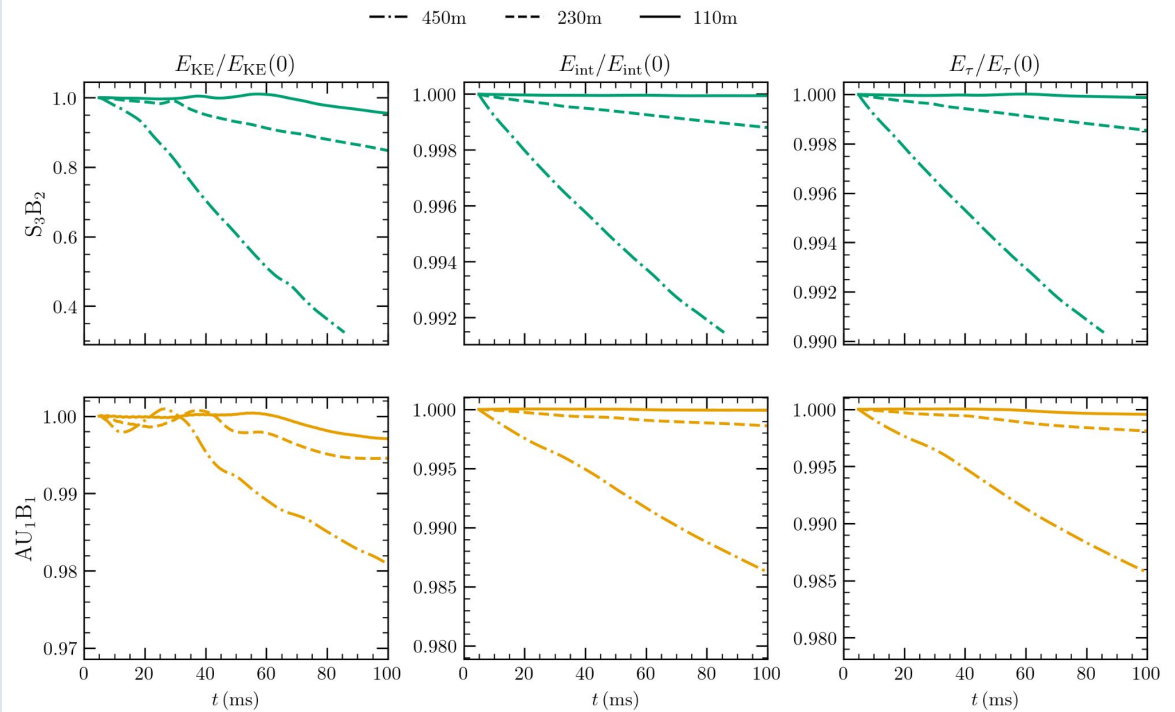


## Convergence

### 110m

< 1% energy conservation. Well converged.

### 230m

~ 0.5–1% level. Acceptable for energetics.

### 450m

Poor: E_KE drops 60% for $S_3B_2$. Insufficient.

**Strategy: 230m for long-duration energetics | 110m HR for instability dynamics, spectra, helicity**